Focusing properties of Gaussian beams by a slab of Kerr-type left-handed metamaterial

Yonghua Hu,[1] Shuangchun Wen,[1,*] Hui Zhuo,[1] Kaiming You,[2] and Dianyuan Fan[1]

[1] *School of Computer and Communication, Hunan University, Changsha 410082, China*
[2] *School of Information Engineering, Wuhan University of Technology, Wuhan 430070, China*
[*] *Corresponding author: scwen@vip.sina.com*

Abstract: Kerr-type left-handed metamaterial (LHM) slab is proved to have an effect of focusing paraxial Gaussian beams and changing their waist radius, as conventional lens can do. The expressions for the focusing distance and the spot radius at the focal point are derived by the variational approach. We show that the incident Gaussian beams can be compressed or expanded by a single Kerr LHM slab, according to the sign of the Kerr nonlinearity and the divergence of the incident beam. Especially, it is demonstrated the focusing properties are significantly tuned by the slab thickness, the beam power and the divergence of the incident Gaussian beam.

OCIS codes: (190.0190) Nonlinear optics; (190.3270) Kerr effect; (350.3618) Left-handed materials.

References and links

1. J. B. Pendry, "Negative Refraction Makes a Perfect Lens," Phys. Rev. Lett. **85**, 3966–3969 (2000).
2. J. B. Pendry, and D. R. Smith, "Reversing light with negative refraction," Phys. Today **57**(6), 37-44 (2004).
3. N. Garcia, and M. Nieto-Vesperinas, "Left-handed materials do not make a perfect lens" Phys. Rev. Lett. **88**, 207403(2002).
4. X. S. Rao, C. K. Ong, "Subwavelength imaging by a left-handed material superlens," Phys. Rev. E **68**, 067601 (2003).
5. D. Maystre, and S. Enoch, "Perfect lenses made with left-handed materials: Alice's mirror?," J. Opt. Soc. Am. A **21**, 122-131(2004).
6. E. Schonbrun, T. Yamashita, W. Park, and C. J. Summers, "Negative-index imaging by an index-matched photonic crystal slab," Phys. Rev. B **73**, 195117 (2006).
7. J. J. Chen, T. M. Grzegorczyk, B. Wu, and J. A. Kong, "Imaging properties of finite-size left-handed material slabs," Phys. Rev. E. **74**, 046615(2006).
8. L. Zhao, and T. J. Cui, "Super-resolution imaging of dielectric objects using a slab of left-handed material," Appl. Phys. Lett. **89**, 141904(2006).
9. M. W. Feise, and Y. S. Kivshar, "Sub-wavelength imaging with a left-handed material flat lens," Phys. Lett. A **334**, 326 (2005).
10. J. J. Chen, T. M. Grzegorczyk, B.-I. Wu, and J. A. Kong, "Limitation of FDTD in simulation of a perfect lens imaging system," Opt. Express **13**, 10840 (2005).
11. A. N. Lagarkov, and V. N. Kissel, "Near-Perfect Imaging in a Focusing System Based on a Left-Handed-Material Plate," Phys. Rev. Lett. **92**, 077401 (2004).
12. V. N. Kissel, and A. N. Lagarkov, "Superresolution in left-handed composite structures: From homogenization to a detailed electrodynamic description," Phys. Rev. B **72**, 085111 (2005).
13. H. L. Luo, W. Hu, Z. Z. Ren, W. X. Shu, and F. Li, "Focusing and phase compensation of paraxial beams by a left-handed material slab," Opt. Commun. **266**, 327-331 (2006).
14. R. Ziolkowski, "Pulsed and CW Gaussian beam interactions with double negative metamaterial slabs," Opt. Express **11**, 662-681 (2003).
15. J. Lu, and S. He, "Numerical study of a Gaussian beam propagating in media with negative permittivity and permeability by using a bidirectional beam propagation method," Microwave Opt. Technol. Lett. **37**, 292-296 (2003).
16. J. A. Kong, B.-I. Wu, and Y. Zhang, "A unique lateral displacement of a Gaussian beam transmitted through a slab with negative permittivity and permeability," Microwave Opt. Technol. Lett. **33**, 136-139 (2002).

#91299 - $15.00 USD Received 3 Jan 2008; revised 14 Mar 2008; accepted 18 Mar 2008; published 24 Mar 2008

17. A. Husakou, and J. Herrmann, "Superfocusing of light below the diffraction limit by photonic crystals with negative refraction," Opt. Express **12**, 6491-6497(2004).
18. P. P. Banerjee, and G. Nehmetallah, "Linear and nonlinear propagation in negative index materials," J. Opt. Soc. Am. B. **23**, 2348-2355 (2006).
19. V. M. Shalaev, "Optical negative-index metamaterials," Nat. Photonics **1**, 41-48 (2007).
20. V. Yannopapas, and N. V. Vitanov, "Photoexcitation-induced magnetism in arrays of semiconductor nanoparticles with a strong excitonic oscillator strength," Phys. Rev. B **74**, 193304 (2006).
21. V. Yannopapas, "Negative refractive index in the near-UV from Au-coated CuCl nanoparticle superlattices," Phys. Stat. Sol. (RRL) **1**, 208-210 (2007).
22. V. Yannopapas, "Artificial magnetism and negative refractive index in three-dimensional metamaterials of spherical particles at near-infrared and visible frequencies," Appl. Phys. A 87, 259-264 (2007).
23. A. A. Zharov, I. V. Shadrivov, and Y. S. Kivshar, "Nonlinear Properties of Left-Handed Metamaterials," Phys. Rev. Lett. **91**, 037401 (2003).
24. I. V. Shadrivov, A. A. Sukhorukov, Y. S. Kivshar, A. A. Zharov, A. D. Boardman, and P. Egan, "Nonlinear surface waves in left-handed materials," Phys. Rev. E **69**, 016617 (2004).
25. P. P. Banerjee, and G. Nehmetallah, "Spatial and spatiotemporal solitary waves and their stabilization in nonlinear negative index materials," J. Opt. Soc. Am. B **24**, A69-A76 (2007).
26. V. M. Agranovich, Y. R. Shen, R. H. Baughman, and A. A. Zakhidov, "Linear and nonlinear wave propagation in negative refraction metamaterials" Phys. Rev. B **69**, 165112 (2004).
27. M. Scalora, M. S. Syrchin, N. Akozbek, E. Y. Poliakov, G. D'Aguanno, N. Mattiucci, M. J. Bloemer, and A. M. Zheltikov, "Generalized Nonlinear Schrödinger Equation for Dispersive Susceptibility and Permeability: Application to Negative Index Materials," Phys. Rev. Lett. **95**, 013902 (2005).
28. I. V. Shadrivov, and Y. S. Kivshar, "Spatial solitons in nonlinear left-handed metamaterials," J. Opt. A: Pure Appl.Opt. **7**, S86-S72 (2005).
29. I. Kourakis, and P. K. Shukla, "Nonlinear propagation of electromagnetic waves in negative-refraction-index composite materials," Phys. Rev. E **72**, 016626 (2005).
30. S. C. Wen, Y. W. Wang, W. H. Su, Y. J. Xiang, X. Q. Fu, and D. Y. Fan, "Modulation instability in nonlinear negative-index material," Phys. Rev. E **73**, 036617 (2006).
31. S.Wen, Y. Xiang, W. Su, Y. Hu, X. Fu, and D. Fan, "Role of the anomalous self-steepening effect in modulation instability in negative-index material," Opt. Express **14**, 1568-1575 (2006).
32. S. Wen, Y. Xiang, X. Dai, Z. Tang, W. Su, and D. Fan, "Theoretical models for ultrashort electromagnetic pulse propagation in nonlinear metamaterials," Phys. Rev. A **75**, 033815 (2007).
33. D. Anderson, M. Bonneal, and M. Lisak, "Variational approach to nonlinear self-focusing of Gaussian laser beams," Phys. Fluids **22**(1), 105-109 (1979).

1. Introduction

In 2000, Pendry introduced the concept of perfect lens [1]. Thereafter, the lensing effect and imaging by a slab of left-handed metamaterial (LHM), which has simultaneously a negative dielectric permittivity and a negative magnetic permeability and thus negative refractive index [2], have attracted extensive interests [3-8]. Because of the negative refractive index, a divergent electromagnetic field from a point source can be refocused by a LHM slab when certain conditions are matched and the entire spectrum of the source can be restored by the LHM slab to obtain an unprecedented subwavelength resolution, which is verified by numerical simulations [9, 10] and experimental measurements [11, 12]. Such an effect has been found to play a significant role in the propagation of electromagnetic wave beam. For example, the phase difference of Gaussian beam caused by the Gouy phase shift in conventional media can be compensated by that in LHMs [13]. There is a unique lateral displacement for a Gaussian beam transmitting through a slab of LHM with an incidence angle [14-16]. Besides, it has been shown that by using a combination of an aperture and a medium slab exhibiting negative refraction, a light beam can be focused to below the diffraction limit [17]. For describing linear propagation in LHMs, partial differential equation is derived and transfer functions are developed [18].

Because of the unique ability for guiding electromagnetic waves, LHMs have been developed quickly in recent years. LHMs were first obtained in the microwave range, now negative refraction up to the optical range can be realized (see, for example, [19]). Structures for low-loss, isotropic LHMs in the optical frequency regime have also been also suggested by Yannopapas et al. [20-22]. Moreover, effective nonlinear electric permittivity and magnetic

#91299 - $15.00 USD Received 3 Jan 2008; revised 14 Mar 2008; accepted 18 Mar 2008; published 24 Mar 2008

permeability in LHMs can be realized by embedding the metallic structure of arrays of wires and split-ring resonators into a dielectric with a nonlinear permittivity that depends on the intensity of the electric field [23]. For LHMs with cubic nonlinear electric response, or Kerr-type LHMs, the interplay between diffraction and nonlinear effect is found opposite to that in conventional Kerr media [24], which leads to the requirement of an effective negative Kerr nonlinearity for the formation of transverse solitary waves in LHMs [25]. This, together with the unique dispersion relation in LHMs, has attracted a lot of researches on related nonlinear effects [26-28]. Besides, modulation instability in LHMs is found unique [29-31], especially the spatial modulation instability doesn't occur in LHMs with positive nonlinearity. These studies suggest that Kerr-type LHMs have a great potential for application in control of light beam propagation.

In this paper, we present an investigation on the focusing properties of Gaussian beams by a LHM slab with a Kerr-type nonlinear polarization. It should be pointed out that the presented study is based on LHMs satisfying the effective medium approximation [22, 24], which treats the medium as homogeneous and isotropic. The Kerr nonlinearity affects the spatial spectra of the beams passing through a medium, and thus the lensing effect of LHMs obtained under linear conditions will be significantly modified by the nonlinear effect.

2. Models

We study the focusing effect of a Gaussian beam by a Kerr LHM slab, which is sketched in Fig. 1. A Gaussian beam propagates along z-axis from the free space D1 through a Kerr LHM slab with a thickness L_{LHM} (region D2), and then in another free space D3. In Fig. 1, $Z_{w,1}$ and $Z_{w,3}$ are the locations of waist of the Gaussian beam in free space D1 and D3, respectively, while $Z_{0,2}$ and $Z_{0,3}$ denote the on-axis coordinates of the front and back surfaces of the Kerr LHM slab, respectively. The Kerr LHM slab is assumed to be lossless and is transversely infinite, and the Gaussian beam is assumed to pass through the interfaces without reflection for simplicity.

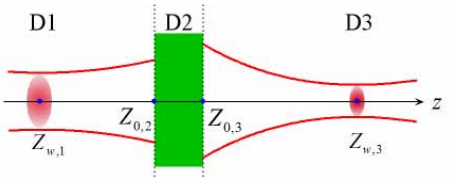

Fig. 1. Propagation model for the focusing of a Gaussian beam by a Kerr LHM slab.

We assume the electric field of the incident Gaussian beam can be written as $\mathbf{E}_1 = \hat{x}A_1(x,y,z)e^{i(kz-\omega t)}$, where ω denotes the circular frequency of the electric field, $A_1(x,y,z)$ is the envelope of the complex amplitude which can be written as

$$A_1(x,y,z) = A_{0,1}\frac{w_{0,1}}{w_1(z)}\exp\left[-\frac{x^2+y^2}{w_1(z)^2}\right]\exp\left[ik_1\frac{x^2+y^2}{2R_1(z)}\right] \tag{1}$$

under the paraxial approximation, i.e., $|\partial A_1/\partial z| \ll k_1 A_1$, and the scalar approximation, where $w_1(z) = w_{0,1}\{1+[(z-Z_{w,1})/L_{R,1}]^2\}^{1/2}$ is the beam spot radius, $A_{0,1}$ and $w_{0,1}$ are the peak amplitude and the spot radius at the beam waist, $R_1(z) = (z-Z_{w,1})\{1+[L_{R,1}/(z-Z_{w,1})]^2\}$ is the curvature radius of the beam phase front, $L_{R,1} = k_1 w_{0,1}^{\ 2}/2$, $k_1 = n_{L,1}2\pi/\lambda_0$, $n_{L,1}= 1$ is the refractive index of free space and λ_0 is the vacuum wavelength of the incident electromagnetic wave. Thus the q parameter of the incident beam is $1/q_1(z) = [1/R_1(z)] - [2/k_1 w_1(z)]$. We

#91299 - $15.00 USD Received 3 Jan 2008; revised 14 Mar 2008; accepted 18 Mar 2008; published 24 Mar 2008

should note here that we assume the paraxial approximation holds in the following theory and calculation.

In the Kerr LHM slab, we use the nonlinear Schrödinger equation

$$i2k_2\frac{\partial A_2}{\partial z}+\left(\frac{\partial^2}{\partial x^2}+\frac{\partial^2}{\partial y^2}\right)A_2+\frac{2{k_2}^2\mu_{rl,2}}{n_{L,2}}C_{NL,2}\left|A_2\right|^2A_2=0 \tag{2}$$

to model the nonlinear propagation of optical beam, which can be obtained from Refs. [27, 30, 32] by neglecting time-dependent effects, where k_2= $n_{L,2}2\pi/\lambda_0$, $n_{L,2}$ is the linear refractive index of the LHM slab, A_2 is the complex envelope of the electric field, $C_{NL,2}=\chi_{p,2}/(2n_{L,2})$ is the nonlinear index coefficient, $\chi_{p,2}$ is the cubic susceptibility, $\mu_{rl,2}$ is the relative magnetic permeability of the LHM slab.

3. Theory analysis

When the Gaussian beam propagates from D1 into D2, it will be transformed by the interface separating D1 and D2. From the expression for the transformation of the q parameter of Gaussian beam in Ref. [18], we can obtain the waist radius $w_{0,2i}$ and the location of the waist $Z_{w,2i}$ of the transformed Gaussian beam as

$$w_{0,2i}=w_{0,1},\ Z_{w,2i}=Z_{0,2}+\left[\left(Z_{w,1}-Z_{0,2}\right)n_{L,2}/n_{L,1}\right], \tag{3}$$

respectively. Then the initial state of the complex envelope of the beam field in the Kerr LHM slab can be written as

$$A_{2i}\left(x,y,Z_{0,2}\right)=A_{0,2i}\frac{w_{0,2i}}{w_{2i}\left(Z_{0,2}\right)}\exp\left[-\frac{x^2+y^2}{w_{2i}\left(Z_{0,2}\right)^2}\right]\exp\left[ik_2\frac{x^2+y^2}{2R_{2i}\left(Z_{0,2}\right)}\right], \tag{4}$$

where $$w_{2i}\left(z\right)=w_{0,2i}\left\{1+\left[\left(z-Z_{w,2i}\right)/L_{R,2i}\right]^2\right\}^{1/2},$$

$R_{2i}\left(z\right)=\left(z-Z_{w,2i}\right)\left\{1+\left[L_{R,2i}/\left(z-Z_{w,2i}\right)\right]^2\right\}$, $L_{R,2i}=k_2{w_{0,2i}}^2/2$, and $k_2=n_{L,2}2\pi/\lambda_0$.

We assume the envelope of the electric field of the beam in the Kerr LHM slab retains Gaussian-shaped and is written as

$$A_2=a_2(z)\exp\left[-\frac{x^2+y^2}{{w_2}^2(z)}+ib_2(z)\left(x^2+y^2\right)+i\varphi_2(z)\right]. \tag{5}$$

By the variational approach [33], we obtain from Eq. (2) the expression for the evolution of beam spot radius in the Kerr LHM slab as

$$w_2\left(z\right)=C_0\sqrt{1+2k_2C_0C_1\left(\frac{z-Z_{0,2}}{k_2{C_0}^2}\right)+\left[K+{k_2}^2{C_0}^2{C_1}^2\right]\left(\frac{z-Z_{0,2}}{k_2{C_0}^2}\right)^2}, \tag{6}$$

where $C_0=w_{2i}(Z_{0,2})=w_1(Z_{0,2})$, $C_1=dw_{2i}(z)/dz\big|_{z=Z_{0,2}}$, $K=4-M\,a_2(z)^2w_2(z)^2$, $M={k_2}^2\mu_{rl,2}C_{NL,2}/n_{L,2}$, $a_2(z)w_2(z)=a_2(Z_{0,2})w_2(Z_{0,2})$ is a constant due to the energy conservation law. Defining the power of the incident beam as $P=(1/2)\varepsilon_0\,|\,n_{L,2}\,|\,\pi a_2(Z_{0,2})^2w_2(Z_{0,2})^2$ and the reference power as $P_{r,2}=\varepsilon_0c\lambda^2/(2\pi\,|\,C_{NL,2}\,|)$, we have

$$K=4\left\{1-\left[-\mu_{rl,2}\,\mathrm{sgn}\left(C_{NL,2}\right)R_P\right]\right\}, \tag{7}$$

#91299 - $15.00 USD Received 3 Jan 2008; revised 14 Mar 2008; accepted 18 Mar 2008; published 24 Mar 2008

where $R_P = P / P_{r,2}$. Further, to reflect the influence of the divergence of the incident beam, we define parameters $\theta_{o,1} = \left(Z_{w,1} - Z_{0,2}\right) / L_{R,1}$ and $\theta_{i,2} = \left(Z_{w,2i} - Z_{0,2}\right) / L_{R,2i}$. Thus, we obtain $\theta_{i,2}=\theta_{o,1}$, $C_0 = w_{0,1}\left(1+\theta_{o,1}^{\ 2}\right)^{1/2}$ and $C_1 = w_{0,1}\left(1+\theta_{o,1}\right)^{-1/2}\left(-\theta_{o,1}\right) / L_{R,2i}$. By these relations, Eq. (6) becomes

$$w_2\left(z\right) = C_0\sqrt{1-4\theta_{o,1}\left(\frac{z-Z_{0,2}}{k_2 C_0^{\ 2}}\right)+\left[K+4\theta_{o,1}^{\ 2}\right]\left(\frac{z-Z_{0,2}}{k_2 C_0^{\ 2}}\right)^2}\ . \tag{8}$$

For simplicity, we consider the case $Z_{w,1}=Z_{0,2}=0$, indicating $C_0=w_{0,1}$ and $\theta_{o,1}=0$. Under these conditions, $b_2\left(z\right)$ and $\varphi_2(z)$ can be obtained by the variational approach and $b_2\left(z\right)$ has the form

$$b_2\left(z\right) = \frac{-K}{2C_0^{\ 2}\left\{1+K\left[\left(z-Z_{0,2}\right)/\left(k_2 C_0^{\ 2}\right)\right]^2\right\}}\left(\frac{z-Z_{0,2}}{k_2 C_0^{\ 2}}\right). \tag{9}$$

Then, at $Z_{0,3}$, we have

$$\left.\begin{aligned} w_2\left(Z_{0,3}\right) &= C_0\sqrt{1+K\left[L_{LHM}\ /\left(k_2 C_0^{\ 2}\right)\right]^2}, \\ b_2\left(Z_{0,3}\right) &= \frac{-K}{2C_0^{\ 2}\left\{1+K\left[L_{LHM}\ /\left(k_2 C_0^{\ 2}\right)\right]^2\right\}}\left(\frac{L_{LHM}}{k_2 C_0^{\ 2}}\right). \end{aligned}\right\} \tag{10}$$

It is clear from equation Eq. (10) that K is a crucial parameter for the output field of the Kerr LHM slab. According to Eq. (7), K can be significantly influenced by the sign of the nonlinear polarization of the LHM slab and the beam power, so we discuss the following three cases: (i), $\chi_{p,2}>0$; (ii), $\chi_{p,2}<0$ and $R_P<1/(-\mu_{rl,2})$; and (iii), $\chi_{p,2}<0$ and $R_P>1/(-\mu_{rl,2})$. For the former two cases, we have $K>0$ and $w_2(Z_{0,3})>C_0$, indicating the beam is self-defocusing in the Kerr LHM slab. For the last case, we obtain that K is smaller than zero and $w_2(Z_{0,3})$ decreases from C_0 as L_{LHM} increases, indicating the beam is self-focusing in the Kerr LHM slab, and so the reference power $P_{r,2}$ can be viewed as the critical power for self-focusing. Thus, the conditions for self-focusing and self-defocusing effects in the Kerr LHM case obtained here are in sharp contrast with their counterparts in the conventional Kerr medium (CKM) case. These results provide arguments for the prediction in Refs. [24, 25]. For the last case, it should be noted that, for certain slab thickness $L_{LHM} = [(k_2 C_0^{\ 2})^2 /(-K)]^{1/2}$, $w_2(Z_{0,3})$ becomes approximately zero. If the slab thickness is close to or bigger than such a value, the beam will be totally self-focused in the Kerr LHM slab and Eq. (10) is no longer valid under such a condition.

In region D3, we can further assume the beam is still Gaussian-shaped. By the boundary conditions at $Z_{0,3}$ similar to those at $Z_{0,2}$, we obtain the expressions for the waist location and the spot radius of the waist of the Gaussian beam as

$$Z_{w,3} = Z_{0,3} + \frac{1}{2}k_3\frac{b_2\left(Z_{0,3}\right)w_2\left(Z_{0,3}\right)^4}{1+b_2\left(Z_{0,3}\right)^2 w_2\left(Z_{0,3}\right)^4},\ w_{0,3} = \frac{w_2\left(Z_{0,3}\right)}{\sqrt{1+b_2\left(Z_{0,3}\right)^2 w_2\left(Z_{0,3}\right)^4}}, \tag{11}$$

respectively. According to above analysis, Eq. (11) holds for four cases: (i) $\chi_{p,2}<0$ and $R_P>1/(-\mu_{rl,2})$ and $L_{LHM} < [(k_2 C_0^{\ 2})^2 /(-K)]^{1/2}$, (ii) $\chi_{p,2}<0$ and $R_P<1/(-\mu_{rl,2})$, and (iii) $\chi_{p,2}>0$ and $R_P<1/(-\mu_{rl,2})$; and (iv), $\chi_{p,2}>0$ and $R_P>1/(-\mu_{rl,2})$. For the first case, we have $Z_{w,3}<Z_{0,3}$, indicating the output beam of the Kerr LHM slab is divergent. For the rest three cases, we have $b_2(Z_{0,3})>0$ and $Z_{w,3}<Z_{0,3}$, indicating the output beam of the Kerr LHM slab is convergent. In the rest three

#91299 - $15.00 USD Received 3 Jan 2008; revised 14 Mar 2008; accepted 18 Mar 2008; published 24 Mar 2008

cases, the effect of the Kerr LHM slab is similar to the effect of a lens. So, in the following part of this paper, we call a Gaussian beam in D3 a focused beam if $Z_{w,3}<Z_{0,3}$ and call this effect as the focusing (or lensing) effect of Kerr LHM slabs on Gaussian beams. Thus, it can be concluded that: (i) both Kerr LHM slabs with a positive nonlinear polarization and those with a negative nonlinear polarization can act as lenses to focus the incident Gaussian beam to a new waist; (ii) for the positive Kerr nonlinearity case, beam focusing happens for both $0<R_P<1/(-\mu_{rl,2})$ and $R_P>1/(-\mu_{rl,2})$ conditions; and (iii) for the negative Kerr nonlinearity case, beam focusing happens for $R_P<1/(-\mu_{rl,2})$ only. For such a focusing effect, the location and the radius of the focal spot are determined by Eq. (11). For convenience, we define the corresponding focusing distance as $L_f = Z_{w,3}-Z_{0,3}$ and especially, define the focusing distance for the case $\theta_{o,1}=0$ as

$$L_{f0} = \frac{1}{2} k_3 \frac{b_2 \left(Z_{0,3}\right) w_2 \left(Z_{0,3}\right)^4}{1+b_2 \left(Z_{0,3}\right)^2 w_2 \left(Z_{0,3}\right)^4}. \tag{12}$$

From Eqs. (11) and (12), it is easy to see that both the focusing distance and the spot radius of the beam waist in D3 are mainly determined by the thickness of the Kerr LHM slab and the ratio of the beam power to the reference power.

3.1 Focusing properties of Gaussian beams by LHM slabs with positive or negative Kerr nonlinearities

Here we analyze the focusing properties of Gaussian beams by Kerr LHM slabs for two cases in this subsection: (i) $\chi_{p,2}>0$, and (ii) $\chi_{p,2}<0$ and $R_P<1/(-\mu_{rl,2})$. Unless specially pointed out, in the following calculations and simulations, we use the following parameters: λ_0 = 1053 nm, $w_2(Z_{0,2})$ = 0.4 mm, R_P = 10, $Z_{w,1} = Z_{0,2}$ = 0, L_{LHM} = 10 cm, $n_{L,2}$ = -1 and $\mu_{rl,2}$ = -1.

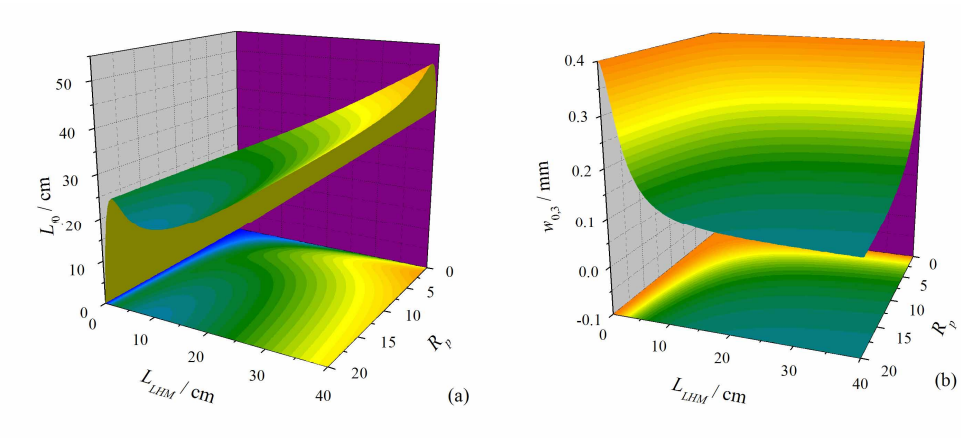

Fig. 2. (a) The focusing distance L_{f0} and (b) the focal spot radius $w_{0,3}$ of the focused Gaussian beam as functions of L_{LHM} and R_P for the case $\chi_{p,2}>0$. (Available in color)

For the case of $\chi_{p,2}>0$, the theoretical predictions for the focusing distance and the waist radius in D3 are shown in Figs. 2(a) and 2(b), respectively. To show the influence of L_{LHM} on L_{f0}, we define the slope of a curve corresponds to certain beam power as $s = \partial L_{f0} / \partial L_{LHM}$. By *s*, we divide the results in Fig. 2(a) into two cases: (i) beam power is some times as high as $P_{r,2}$, e.g. R_p is about 5, and (ii) power ratio is large, e.g. R_p is about 18. For case (i), *s* is always positive and L_{f0} keeps increasing as L_{LHM} increases. For case (ii), though generally positive, *s* can be negative in a certain value range of L_{LHM} where L_{f0} decreases as L_{LHM} increases. It should also be noted that *s* approaches one finally in both cases. Figure 2(b)

#91299 - $15.00 USD Received 3 Jan 2008; revised 14 Mar 2008; accepted 18 Mar 2008; published 24 Mar 2008

shows that the waist radius in D3 is inversely proportional to both the slab thickness and the beam power. Thus, the same focal spot radius can be obtained by changing the incident beam power or the thickness of the LHM slab. Besides, for Gaussian beams with very high power, evidently focusing effect can be obtained by a thin LHM slab.

For the case of $\chi_{p,2}<0$ and $R_P<1/(-\mu_{rl,2})$, the theoretical predictions for the focusing distance and the waist radius in D3 are shown in Fig. 3. In this case, for each slab thickness larger than zero, the focusing distance L_{f0} decreases as the beam power increases, and the variation of the waist radius $w_{0,3}$ in D3 with the beam power looks like a parabola. These are different from those shown by Fig. 2. Moreover, for Fig. 3(b), it should be noted that the waist radius in D3 is larger than the incident beam waist, which is contrary to that shown by Fig. 2(b), and that the variation in absolute waist radius is smaller when compared to that in Fig. 2(b).

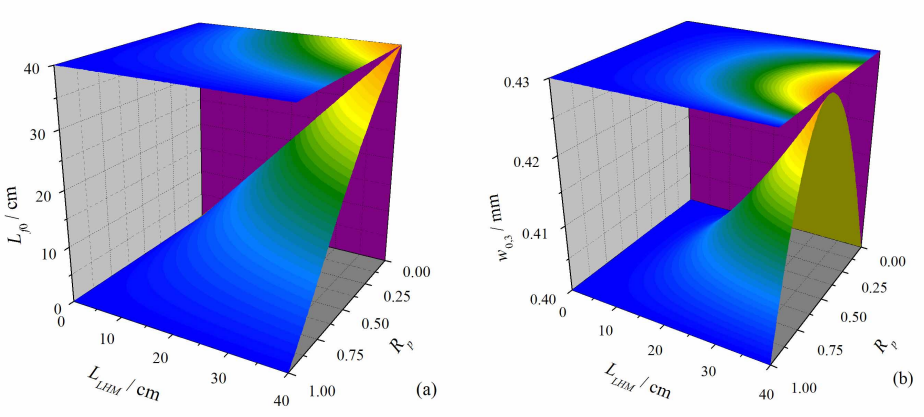

Fig. 3. (a) The focusing distance L_{f0} and (b) the focal spot radius $w_{0,3}$ of the focused Gaussian beam as functions of L_{LHM} and R_P for the case $\chi_{p,2}<0$ and $R_P<1/(-\mu_{rl,2})$. (Available in color)

Such a focusing effect is originated from the anomalous interaction between the diffraction and nonlinear effect in the Kerr LHM slab. In LHMs, the wavenumber is negative. Thus, for the first case, the phase shift caused by the positive nonlinear polarization and that caused by diffraction are positive and so the nonlinear effect enhances the diffraction effect in the Kerr LHM. For the second case, the phase shift caused by the negative nonlinear polarization is negative and so the nonlinear effect suppresses the diffraction effect in the Kerr LHM. Combining Eqs. (5) and (10), we obtain the spatial chirp of the Gaussian beam at $Z_{0,3}$ is $G = -K\,L_{LHM}/(k_2 C_0^{\,2})$. Considering the half-width (at 1/*e*-intensity point) of the spatial spectrum of Gaussian beam satisfies $\Delta\Omega = (1+G^2)^{1/2}/w$, where w is the half-width (at 1/*e*-intensity point) of the beam spot, we obtain from Eqs. (4), (5) and (10) the half-width of the spatial spectrum at the back surface of the slab:

$$\Delta\Omega_{Z_{0,3}} = \Delta\Omega_{Z_{0,2}}\left[1+K^2\left(\frac{L_{LHM}}{k_2 C_0^{\,2}}\right)^2\right]\Big/\left[1+K\left(\frac{L_{LHM}}{k_2 C_0^{\,2}}\right)^2\right]. \qquad (13)$$

From Eq. (13), it can be inferred that $\Delta\Omega_{Z_{0,3}} > \Delta\Omega_{Z_{0,2}}$ and $\Delta\Omega_{Z_{0,3}} < \Delta\Omega_{Z_{0,2}}$ for the first case and the second case, respectively. On the other hand, Gaussian beams with broader spatial spectrum have smaller waist radius, so, for the first case and the second case, the waist radius in D3 are smaller and larger than that of the incident beam, respectively.

Moreover, it should be noted that the magnetic permeability of LHM slabs can quantitatively modify the above-mentioned influence of the beam power (see Eq. (7)). This is

#91299 - $15.00 USD Received 3 Jan 2008; revised 14 Mar 2008; accepted 18 Mar 2008; published 24 Mar 2008

very important for the second case, especially when the beam power equals approximately to the reference power, where small variation in permeability can change the convergent beam in D3 into a divergent one, or vice versa.

3.2 Comparisons with the linear LHM slab case and the conventional Kerr medium slab case

At first, let us consider the case that the LHM slab in Fig. 1 is a linear medium. In this case, it is easy to obtain $L_{f0} = n_{L,2}L_{LHM} / n_{L,1}$, which is just related to the slab thickness and the refractive index, and $w_{0,3} = w_{0,1}$, which is not related to the slab thickness [1, 13]. When compared to this case, the above-mentioned lensing effect of Gaussian beam by Kerr LHM slab has more diverse results: (i) The waist of the beam in D3 can be larger or smaller than that of the incident beam; (ii) The focusing distance can also be larger or smaller than the slab thickness; (iii) Both the new waist radius and the focusing distance are functions of the beam power, the thickness, the magnetic permeability and the nonlinear polarization of the slab.

Moreover, conventional lenses can compress or expand Gaussian beams passing through them. From this point of view, Kerr LHM slabs act as conventional lenses more than linear ones do.

We now consider the case that the Kerr LHM slab in Fig. 1 is substituted with a CKM slab. For this case, the above obtained expressions are also valid by just setting $\mu_{rl,2}$=1 and $n_{L,2}$>1. For incident Gaussian beams with $\theta_{o,1}$=0, there are two cases: (i) they will be self-defocused for $\chi_{p,2}$<0 or for $\chi_{p,2}$>0 and R_P<1, and (ii) they will be self-focused for $\chi_{p,2}$>0 and R_P>1. Then, it can be inferred from Eq. (10) that: (i) for the former case, $b_2(Z_{0,3})$<0 and the beam in D3 is divergent; (ii) for the latter case, if the conditions for $w_2(Z_{0,3})$>0 are satisfied, $b_2(Z_{0,3})$>0 and the output beam of the CKM slab is convergent, indicating the beam can also be focused in D3. However, for the latter case, the beam suffers from modulation instability and thus filamentation may occur when there is small-scale modulation. For convenience, we assume that the waists of the incident beams are identical. Then, we find the main differences between the focusing properties of Gaussian beams by a Kerr LHM slab and those by a CKM slab case to be the following:

(i) For beams with lower power, i.e. R_P<1/(-$\mu_{rl,2}$), both LHM slabs with positive nonlinear polarization and those with negative nonlinear polarization has the lensing effect on them;

(ii) For $\chi_{p,2}$>0, beams don't suffer from modulation instability or filament formation in Kerr LHMs, as shown in Ref. [30];

(iii) Under the same beam and slab conditions, the focusing effect of the Kerr LHM slab with $\mu_{rl,2}$=-1 is not as strong as that of the CKM slab. The reason is that the power density in the Kerr LHM slab is smaller than that in the CKM slab, which weakens the nonlinear effect, and thus the focal spot size in D3 from the Kerr LHM slab is larger than that from the CKM slab.

4. Numerical simulations

Besides the factors discussed in the previous section, it is clear from Eq. (8) that the initial status of the incident beam also modifies the focusing properties. In this section we discuss the influence of the initial status of the beam on the focusing properties numerically. We first consider a special case that the waist of the incident Gaussian beam is at the front surface of the LHM slab, and then a general case that the waist of the incident Gaussian beam is before or behind this surface. We simulate the propagation of beam focusing by Kerr LHM slab through using the standard split-step Fourier algorithm. The properties of the Kerr LHM slab used for simulation consist with the theory in the previous section. For propagation in region D2, Eq. (2) is used. In region D3, a similar equation to Eq. (2) is used, with the nonlinear term removed. For the latter, all the quantities are replaced with those for free space. The step width is 1 mm in the Kerr LHM (also D2) slab and 1 cm in D3. If not especially pointed out, we use the default parameters given in section 3.1 and set $\chi_{p,2}$>0 and R_P>1/(-$\mu_{rl,2}$).

#91299 - $15.00 USD Received 3 Jan 2008; revised 14 Mar 2008; accepted 18 Mar 2008; published 24 Mar 2008

4.1 $\theta_{o,1} = 0$

The results for the radius of the beam waist in D3 and those for the focusing distance are shown in Figs. 4(a) and 4(b), respectively. In Fig. 4(a), good agreement can be seen between theoretical prediction and numerical results. Moreover, both theoretical prediction and numerical results show that either increasing the thickness of the Kerr LHM slab or increasing the incident beam power lead to a smaller waist when other conditions are the same. The theoretical and simulated results in Fig. 4(b) also reflect the same trend in the variations of the respective quantities. The quantitative differences between the theoretical and the simulated results in Fig. 4 are originated from the approximations introduced in the variational approach.

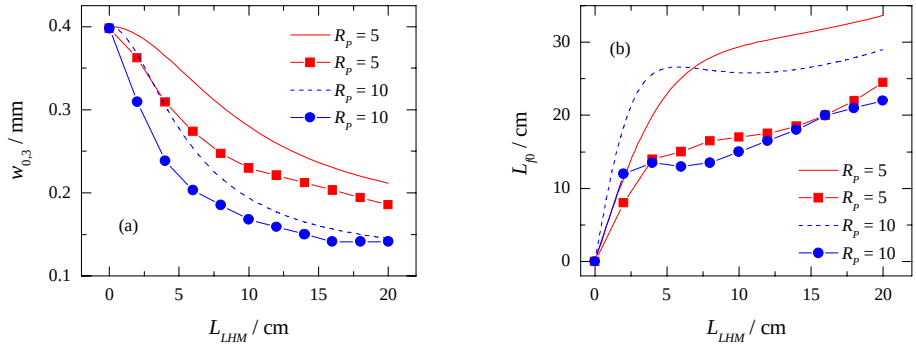

Fig. 4. (a) The spot radius of the beam waist in D3 and (b) the focusing distance versus the thickness of the Kerr LHM slab. The solid curve and the dashed curve are theoretical predictions; the rectangular-dotted curve and the circular-dotted curve are simulated results.

4.2 $\theta_{o,1} \neq 0$

According to its definition, $\theta_{o,1}$ depends on the convergence/divergence of incident Gaussian beams, i.e. for convergent incident beams, $\theta_{o,1}>0$, and for divergent incident beams, $\theta_{o,1}<0$. On the other hand, it is easy to infer from Eq. (4) that $\theta_{o,1}$ represents the linear spatial chirp of incident Gaussian beams of the Kerr LHM slab. To see the influence of $\theta_{o,1}$, we keep the spot radius at $Z_{0,2}$ fixed for simplicity. In addition, in the Kerr LHM slab, the thickness of the slab also plays an important role in this case according to Eq. (8). Thus, we discuss the following two sub-cases: one is for a thick slab (L_{LHM}=10 cm); the other is for a thin slab (L_{LHM}=4 cm).

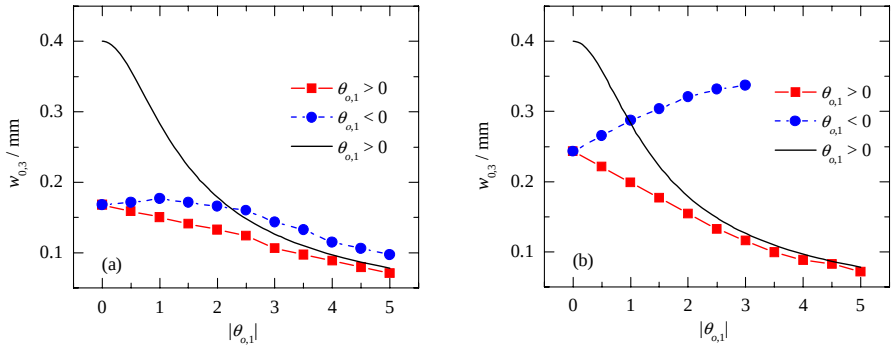

Fig. 5. The focal spot radius versus $|\theta_{o,1}|$. The thicknesses of Kerr LHM slabs in (a) and (b) are 10 cm and 4 cm, respectively. In both figures, the solid curves are the theoretical results for L_{LHM}=0, where $w_{0,3} = w_{0,1}$, other curves are simulated results.

#91299 - $15.00 USD Received 3 Jan 2008; revised 14 Mar 2008; accepted 18 Mar 2008; published 24 Mar 2008

Numerical results for default conditions are shown in Fig. 5, where $|\Delta\theta_{o,1}|=0.5$. In this figure, it should be noted that the solid curve also represents the transform limited waist radius of the incident beam. Figure 5(a) shows the results for the thick-slab case. For $\theta_{o,1}>0$, the beam waist radius decreases as $\theta_{o,1}$ increases. For $\theta_{o,1}<0$, as $|\theta_{o,1}|$ increases, the beam waist radius increases at first and then decreases after reaching the maximum. This shows that irrespective of the initial beam divergence/convergence the incident beam can be focused by thick Kerr LHM slabs under certain conditions. When compared to the values shown by the solid curve, the numerical results for $\theta_{i,2}>0$ are always smaller, while those for $\theta_{i,2}<0$ can also be bigger when $|\theta_{o,1}|$ is big enough. For the thin-slab case shown by Fig. 5(b), for the case $\theta_{o,1}>0$, the variation trend of $w_{0,3}$ is the same as that in Fig. 5(a), but for the case $\theta_{i,2}<0$, $w_{0,3}$ keeps increasing as $|\theta_{i,2}|$ increases and finally the beam becomes divergent in D3.

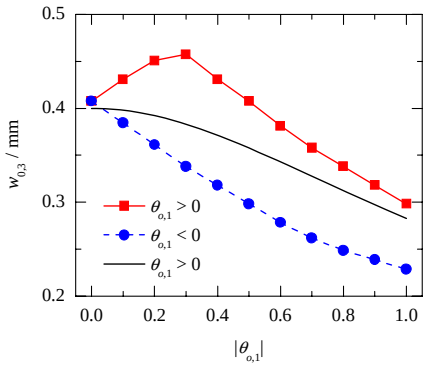

Fig. 6. The focal spot radius versus $|\theta_{o,1}|$ for $\chi_{p,2}<0$. Solid curve, as that in Fig. 5, is the theoretical result for $L_{LHM}=0$, where $w_{0,3} = w_{0,1}$, other curves are simulated results. $|\Delta\theta_{o,1}|=0.1$.

For focusing effect in the $\chi_{p,2}<0$ and $0<R_P<1$ case, however, because the absolute increment of beam waist radius is relatively small (see Fig. 3(b)), we set $R_P=0.5$ and $L_{LHM}=40$ cm to obtain evident results. The influence of $\theta_{o,1}$ on the new beam waist is presented in Fig. 6. It is clear that because of $\theta_{o,1}$, the difference between $w_{0,3}$ and $w_{0,1}$ can be larger than the $\theta_{o,1}=0$ case. For the case $\theta_{o,1}>0$, $w_{0,3}$ increases at first and then decreases as $|\theta_{o,1}|$ increases and it always bigger than $w_{0,1}$; for the case $\theta_{o,1}<0$, $w_{0,3}$ decreases as $|\theta_{o,1}|$ increases and basically smaller than $w_{0,1}$. Comparing Fig. 6 to Fig. 5(a), it is easy to find that the effects of the convergence/divergence of incident Gaussian beams in these two cases are opposite to each other.

The physical mechanism for these cases is, like that discussed for the case $\theta_{o,1}=0$ in the previous section, also the interaction between the diffraction and the nonlinearity. But here the effect of the initial spatial chirp should be included. Here, we take the $\chi_{p,2}>0$ condition for example. For the case $\theta_{o,1}>0$, the total spatial chirp of the output beam of the Kerr LHM slab is greater than that in the case $\theta_{i,2}=0$. For the case $\theta_{i,2}<0$, because the initial spatial chirp has opposite sign to the spatial chirp aroused by the co-effect of diffraction and nonlinearity, it will be cancelled by the latter in the initial stage of propagation in the slab. Thus, as shown by Eq. (8), the beam spot radius is initially decreasing in the slab and the focusing effect is weakened. For similar reasons, the results for $\theta_{o,1}\neq0$ are related to the slab thickness. For the 10 cm slab case, the negative initial chirps are totally cancelled in less than 10 cm, so the beam can always be focused in the value range of $\theta_{o,1}$ in Fig. 5. For the 4 cm slab case, for the case $|\theta_{o,1}|$ is relatively smaller, the initial chirps can be totally cancelled in less than 4 cm and the beam can always be focused, while for the case $|\theta_{o,1}|$ is relatively larger, the initial negative chirps cannot be totally cancelled in the slab.

#91299 - $15.00 USD Received 3 Jan 2008; revised 14 Mar 2008; accepted 18 Mar 2008; published 24 Mar 2008

5. Conclusion

We have investigated the propagation of Gaussian beams through a single Kerr LHM slab and found Kerr LHM slabs can act as lenses to focus Gaussian beams. By the variational approach, we have derived the analytical expressions for the focusing distance and the spot radius at the beam waist. By these expressions, the dependence of the focusing distance and the waist radius at the focal point on the slab thickness and the beam power is identified. We found that Gaussian beams can be focused in two cases: one is that the nonlinear polarization of LHM slabs is positive; the other is that the nonlinear polarization of LHM slabs is negative and the beam power is smaller than the effective critical power for self-focusing in Kerr LHMs. In the case the Kerr LHM slabs have positive (negative) nonlinear polarization, the focusing distance can be longer (shorter) than the imaging distance obtained in the linear LHM slab case, and the waist radius at the focal point can be much smaller (larger) than that of the incident beam. Especially, for a thin Kerr LHM slab with positive nonlinear polarization, when the beam power is very high, evident beam compressing effect can be seen and the focusing distance is much larger than the thickness of the slab. This is in sharp contrast with the CKM slab case and the linear LHM slab case. Besides, the convergence/divergence, or spatial chirp, of incident beam is found important for modifying focusing properties. For LHM slabs with positive nonlinear polarization, initially positive spatial chirp can stimulate but the negative one can suppress, even eliminate the focusing effect; for LHM slabs with negative nonlinear polarization, however, the result is reversed.

Acknowledgments

This work was partially supported by the National Natural Science Foundation of China (Grant Nos. 10674045, 10576012, and 60538010), and the program of the Ministry of Education of China for New Century Excellent Talents in University.

#91299 - $15.00 USD Received 3 Jan 2008; revised 14 Mar 2008; accepted 18 Mar 2008; published 24 Mar 2008